Solid State Phenomena
ISSN: 1662-9779, Vol. 362, pp 89-96
doi:10.4028/p-z5xalB

Submitted: 2023-09-30
Accepted: 2024-05-20
Online: 2024-08-27

Characterization of Growth Sectors in Gallium Nitride Substrate Wafers

Yafei Liu[1,a*], Shanshan Hu[1,b], Zeyu Chen[1,c], Qianyu Cheng[1,d], Ming Kit Cheng[2,e], Wei Zhao[2,f], Temel Buyuklimanli[2,g], Balaji Raghothamachar[1,h] and Michael Dudley[1,i]

[1]Department of Materials Science and Chemical Engineering, Stony Brook University, Stony Brook, NY 11794, USA

[2]Eurofins, EAG Laboratories, Sunnyvale, CA 94086, USA

[a]yafei.liu@stonybrook.edu, [b]shanshan.hu@stonybrook.edu, [c]zeyu.chen@stonybrook.edu, [d]qianyu.cheng@stonybrook.edu, [e]MingKitCheng@eurofinseag.com, [f]WeiZhao@eurofinseag.com, [g]Temel@eurofinseag.com, [h]balaji.raghothamachar@stonybrook.edu, [i]michael.dudley@stonybrook.edu

Keywords: Growth Sectors, HVPE, X-Ray Topography, Impurities

Abstract. During crystal growth processes, growth sectors are formed due to growth along different crystallographic directions. Although the crystal structure in the different growth sectors is unchanged, strain induced topography contrast is observed by synchrotron X-ray topography. In this study, synchrotron monochromatic beam X-ray topography (SMBXT), synchrotron X-ray plane wave topography (SXPWT), scanning electron microscopy (SEM), transmission electron microscopy (TEM), and secondary ion mass spectrometry (SIMS) are used to characterize growth sectors in gallium nitride (GaN) substrate wafers grown by patterned hydride vapor phase epitaxy (HVPE). The SMBXT images reveal the boundaries of $\{000\bar{1}\}$ and $\{11\bar{2}2\}$ type growth sectors. Strain maps generated from SXPWT shows that the out-of-plane strains in different growth sectors have a difference of the order of 10^{-5}. SEM images from SE2 signal shows no contrast of growth sector boundaries while images from Robinson detector (RBSD) show different growth sectors as different grey scale contrast, indicating a strain effect. SIMS analysis shows that the different oxygen impurity levels in the growth sectors, which is the origin of the strain. A formation mechanism of growth sectors in patterned HVPE grown GaN wafers is proposed.

Introduction

Power electronic devices are widely used in AC-DC energy conversion applications. As the power and frequency increase, the energy loss during switching becomes more and more significant. Wide band gap semiconductor materials like silicon carbide (SiC) and gallium nitride (GaN) could potentially replace silicon in power electronics. While SiC is increasingly adopted in the automotive sector, the application of GaN in high-performance power electronic devices has been limited by the quality and availability of bulk GaN substrates. Several methods have been developed to grow bulk GaN crystals, including physical vapor transport (PVT) [1, 2], Na-flux [3], ammonothermal [4, 5], and hydride vapor phase epitaxy (HVPE) [6]. Additionally, to further reduce the dislocation densities, patterned HVPE growth methods have also been developed [7]. Among these different growth methods, ammonothermal and patterned HVPE growth methods have shown promise in producing high-quality GaN crystals for use in power devices [8-10]. Ammonothermal-grown GaN has an overall low dislocation density of 1000 cm^{-2}, while patterned growth can concentrate dislocations into small areas, leaving the rest of the crystal relatively dislocation-free ($< 10^2$ cm^{-2}). Besides dislocations, the overall homogeneity of these wafers is also important for devices.

In the patterned HVPE growth method, growth sectors have been reported to exist due to growth along different crystallographic directions [11]. However, no comprehensive characterization study has been conducted of these sectors. Understanding the microstructure and nature of the growth sectors is important for device fabrication as the inhomogeneities will likely be replicated into active regions. In this study, investigation in the microstructure and nature of the growth sectors in

conducted by various characterization techniques including synchrotron monochromatic beam X-ray topography (SMBXT) [12], synchrotron X-ray plane wave topography (SXPWT, previously known as synchrotron X-ray rocking curve topography) [13], scanning electron microscopy (SEM), transmission electron microscopy (TEM), and secondary ion mass spectrometry (SIMS). A formation mechanism of such growth sectors is proposed.

Experimental

A GaN substrate wafer grown by patterned HVPE method was characterized by SMBXT and SXPWT at the beam line 1-BM at Advanced Photon Source (APS) in Argonne National Laboratory (ANL). Grazing incidence SMBXT images from the $11\bar{2}4$ reflection (39.13° to c-plane) was recorded by high resolution Agfa Structurix D3sc X-ray films. SXPWT data from 0004 reflection was recorded by an ANDOR Neo 5.5 sCMOS camera, and the setup realized a resolution of 2.5 μm per pixel. MATLAB R2023a software was used to calculate the strain maps from the SXPWT data.

SEM images were taken by a Zeiss LEO 1550 field emission SEM in the Department of Materials Science and Chemical Engineering at Stony Brook University. TEM work was done on a JEOL 2100F system at Center for Functional Nanomaterials (CFN) in Brookhaven National Laboratory (BNL). SIMS analysis was in collaboration with EAG laboratories.

Results and Discussion

Previous SMBXT work on characterization of GaN substrates grown by patterned HVPE method has shown that periodically distributed strain centers can be observed (Fig. 1). From the enlarged image shown in Fig. 2, low dislocation density can be found in the regions between the strain centers. However, domains with enclosed shape contrast are observed. The domain boundaries have linear contrast but different from basal plane dislocations (BPDs). No significant difference in the contrast inside and outside of the domain boundary can be observed in the grazing incidence topograph. With the diffraction behavior of X-rays across the entire wafer being the same, two domains have the same crystal lattice structure.

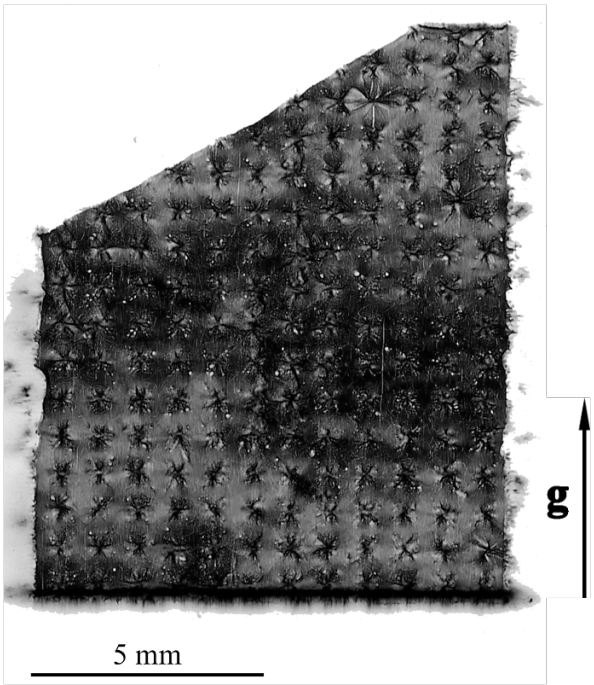

Fig. 1. SMBXT image (E=9.37 kev, $\boldsymbol{g} = 11\bar{2}4$) of a patterned HVPE grown GaN substrate. Strain centers can be observed as a four-fold pattern across the whole sample.

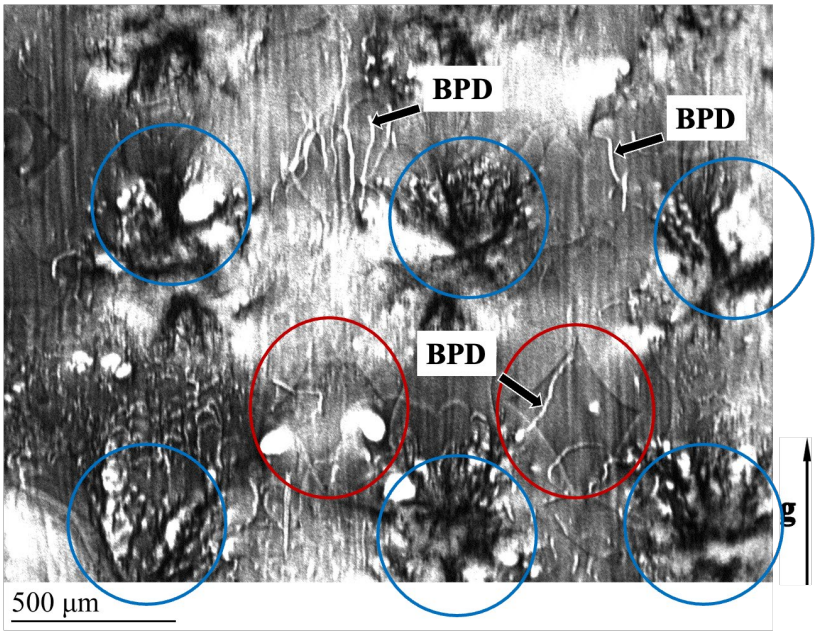

Fig. 2. SMBXT image (E=9.37 kev, $\boldsymbol{g} = 11\bar{2}4$) of a patterned HVPE grown GaN substrate. Low dislocation density can be found between the strain centers marked by blue circles, but enclosed domain shapes are observed and marked by red circles. The domain boundaries have linear contrast but different from BPDs marked by black arrows.

To confirm the lattice structures, High-Resolution TEM (HRTEM) was conducted. Two cross-sectional TEM samples in the $11\bar{2}0$ planes were prepared by focused ion beam (FIB) method from both inside and outside the domain region. No difference in lattice structure is observed between Fig. 3 (a) and Fig. 3 (b) as they both follow the ABAB… stacking sequence of the 2H type structure.

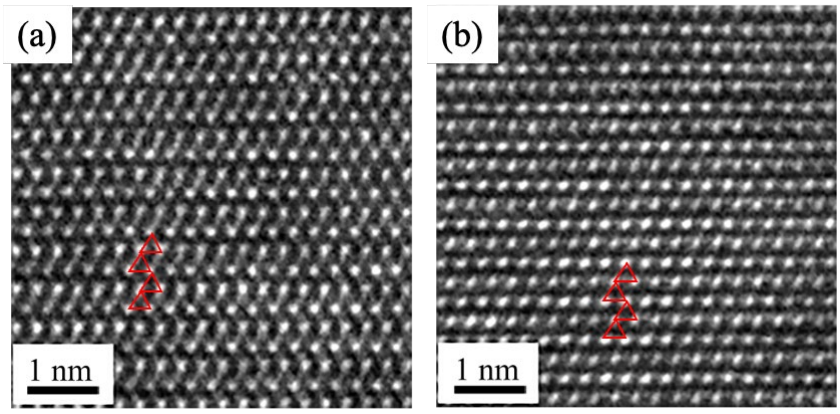

Fig. 3. HRTEM images take from $(11\bar{2}0)$ samples of (a) inside the domain and (b) outside the domain. Both stacking sequences follow ABAB…, which indicates a typical 2H structure.

SXPWT was conducted on the same sample. According to DuMond diagrams [14] shown in Fig. 4, the setup of SMBXT gives an X-ray incident beam with a full width at half maximum (FWHM) of 6.5 arc seconds. On the other hand, SXPWT setup can give a much smaller FWHM down to 0.48 arc seconds, due to the incorporation of the highly asymmetric Si (331) beam conditioner as the second crystal after the double Si (111) monochromators. This setup can achieve a very high strain sensitivity of the order of 10^{-6}. This nearly plane wave X-rays help reveal as shown in Fig. 5 that the operative Bragg angle inside the domains is slightly different from those around the domains. The difference is around 30 arc seconds. Strain and tilt maps were generated by deconvoluting the SXPWT data [13] to check if the peak shift is from strain or tilt effect of the lattice. In the strain map shown in Fig. 6 (a), the domains are clearly observed as regions with compressive strain values in the magnitude of 10^{-5}. However, in Fig. 6 (b), the same domains show no difference in tilt values. This means that the Bragg peak shift of the domain regions is contributed by pure strain.

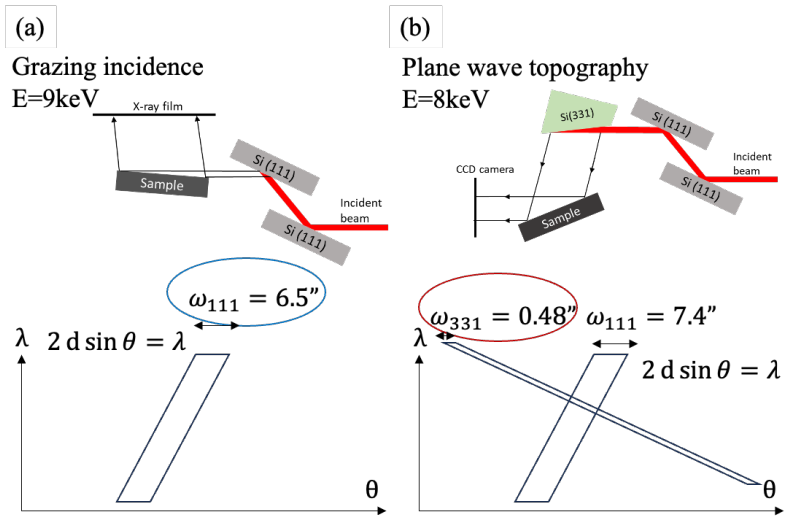

Fig. 4. Experimental setup and the corresponding DuMond diagram of (a) grazing incidence geometry and (b) plane wave topography. The addition of Si (331) beam conditioner significantly decreases the FWHM of the beam from 6.5” to 0.48”.

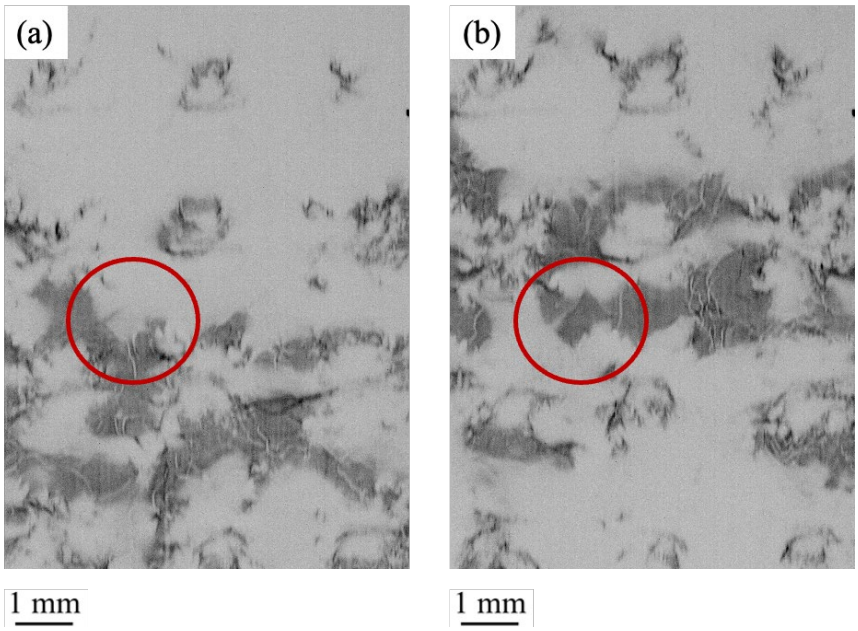

Fig. 5. Images recorded by SXPWT of the same area. The marked region shows a domain area that has a different Bragg angle from the surrounding regions. The angular rotation of the sample from (a) to (b) is around 30 arc seconds.

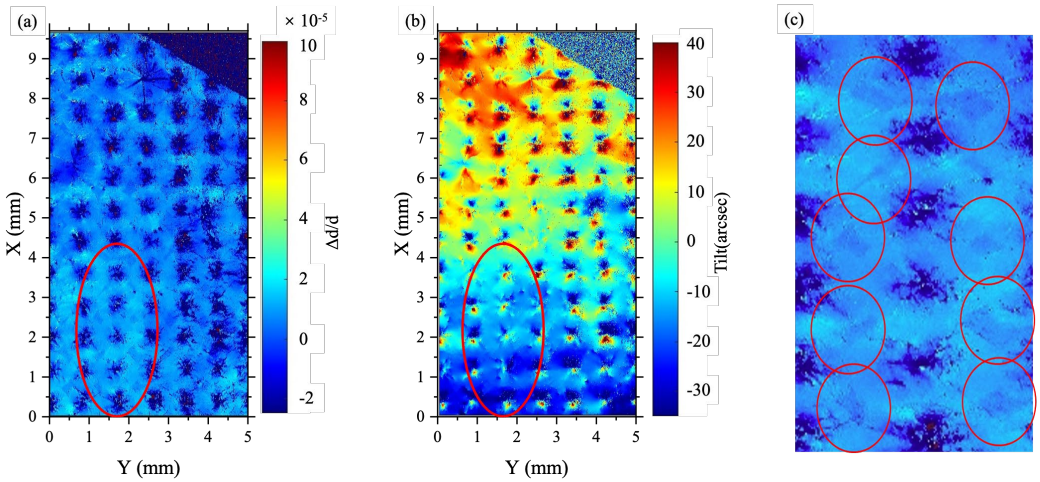

Fig. 6. (a) Strain map and (b) tilt map generated from SXPWT (E=8.05kev, $\boldsymbol{g} = 0008$). The domain features are visible in the strain map but not in the tilt map, which means that the Bragg peak shift in the domain region is from pure strain. (c) is the magnified image, giving a clearer view of the domain features with compressive strain in the level of 10^{-5}.

To further investigate the nature of the domains, SEM was conducted. Fig. 7 shows the image comparison of the same region with different detectors. The domain features cannot be observed in the SE2 mode. However, the RBSD mode reveals the domain regions as dark contrast. These domain regions are confirmed to be the same features observed in images taken by SMBXT and strain maps from SXPWT, shown in Fig. 8.

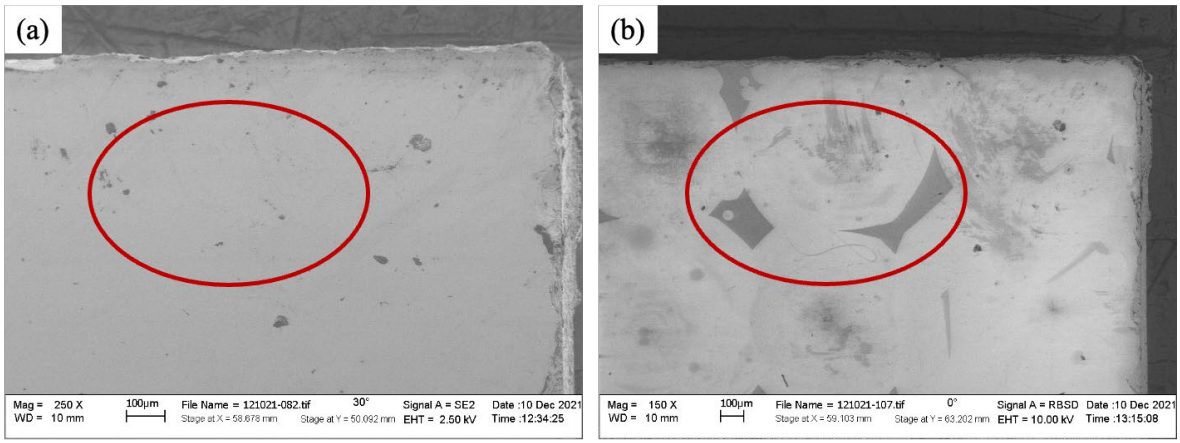

Fig. 7. SEM image of the same area of the patterned HVPE grown GaN substrate with (a) SE2 detector and (b) RBSD detector. The domain contrast only shows under the RBSD detector, which means that they are not surface feature and are strain related.

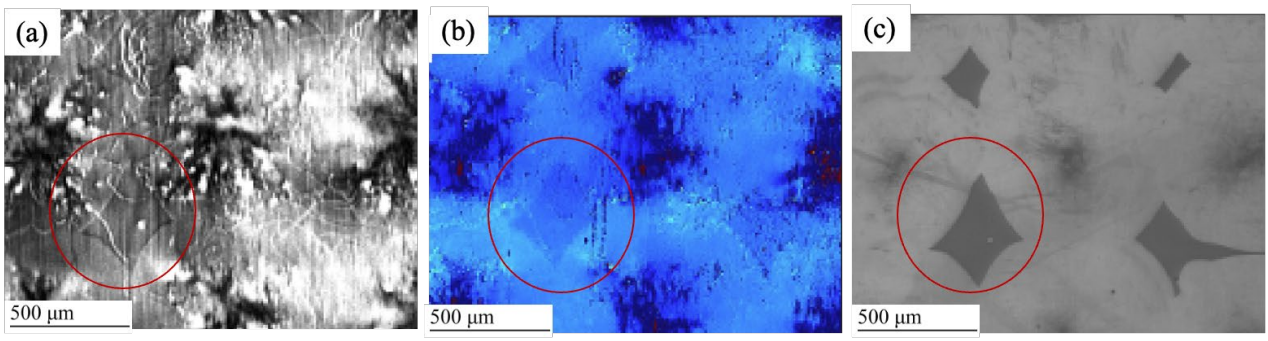

Fig. 8. Correlation of the same feature in the (a) SMBXT image, (b) strain map from SXPWT, and (c) SEM image under RBSD mode.

In HVPE grown GaN materials, growth sectors have been reported to exist due to growth along different crystallographic directions [11]. Because the impurity incorporation rates along different growth directions are different, SIMS analysis was adopted to confirm the nature of the domain features. Oxygen is the most common impurity element in HVPE growth. The concentrations of oxygen were obtained from both inside and outside of the domain area. Fig. 9 shows that the oxygen concentration from outside of the domain is at the level of 10^{18} atoms/cm^3, while the oxygen concentration level is below the detection limit of 10^{15} atoms/cm^3 inside the domain. This result demonstrates that the two types of domains separated by the boundaries shown in SMBXT images are different growth sectors.

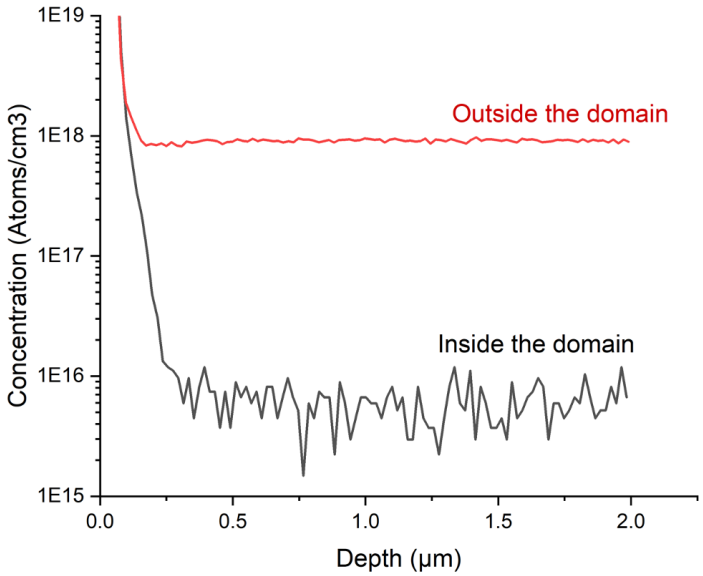

Fig. 9. SIMS analysis on the oxygen impurity concentration shows the difference from inside and outside of the domain region. The oxygen impurity level inside the domain is below the detection limit.

The origin of such growth sectors lies in the HVPE growth process shown in Fig. 10. In the patterned HVPE growth, a pattern of inverted polarized materials is first deposited on the growth template (Fig. 10 (a)). Growth rate on top of the inverted polarized materials is lower than the other areas, as shown in Fig. 10 (b). From a study of growth rates along different directions by kinetic Wulff plots [15], $\{11\bar{2}2\}$ type facets are predicted to form. Growth on both $(000\bar{1})$ and $\{11\bar{2}2\}$ type facets will result in different growth sectors separated by growth sector boundaries (Fig. 10 (c)). The 6 $\{11\bar{2}2\}$ facets have a hexagonal outline when viewed from the top, as shown in Fig. 10 (d). As the four-fold $\{11\bar{2}2\}$ sectors expand, the $(000\bar{1})$ sectors become diamond shapes shown in Fig. 8. Despite the difference in strain between the growth sectors being small, the growth sector boundaries are mostly located in the low dislocation density regions, which are the target locations for power device fabrication. The small strain difference near the growth sector boundaries can potentially induce lattice defects during epitaxy, ion implantation, and annealing thereby influencing the performance of the devices fabricated in those regions.

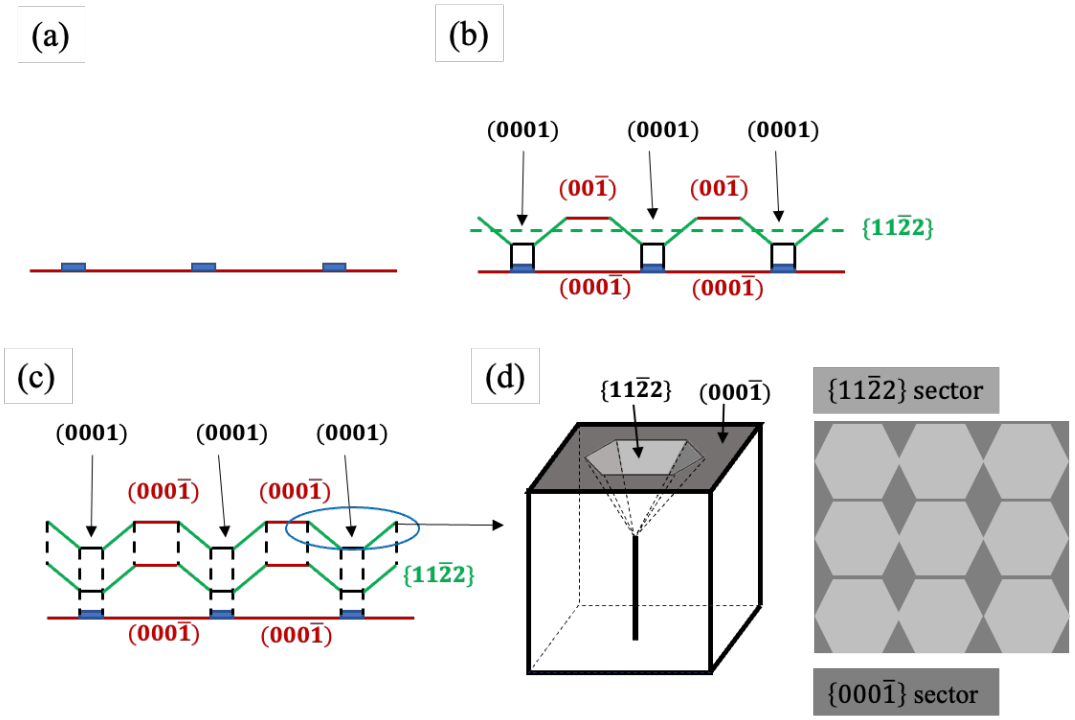

Fig. 10. Formation of the growth sectors during growth. (a) A pattern of inverted polarized materials is first deposited on the growth template. (b) Growth rate on top of the inverted polarized materials is lower than the other areas. $\{11\bar{2}2\}$ type facets form. (c) Growth on both $(000\bar{1})$ and $\{11\bar{2}2\}$ type facets will result in different growth sectors separated by growth sector boundaries. (d) The 6 $\{11\bar{2}2\}$ facets have a hexagonal outline when viewed from the top. As the four-fold $\{11\bar{2}2\}$ sectors expand, the $(000\bar{1})$ sectors become diamond shapes.

Summary

Growth sectors are observed and identified in patterned HVPE grown GaN substrates by SMBXT, SXPWT, SEM, TEM, and SIMS. Different growth sectors are formed by $(000\bar{1})$ and $\{11\bar{2}2\}$ type facets during growth. The growth sector boundaries show as linear features in SMBXT. The strain levels are different in the growth sectors, and the difference is quantified by the strain maps calculated from SXPWT data. The strain difference is a result of different oxygen impurity concentrations, which are measured in different growth sectors by SIMS analysis. The formation mechanism and the nature of the growth sectors are explained. Attention should be paid to these growth sector boundaries because the performance of devices fabricated on top of them can be affected.

Acknowledgement

The X-ray topography work is supported by ARPA-E through PNDIODES program (Project Director: I. Kizilyalli). Synchrotron X-ray topographs were recorded using the resources of the Advanced Photon Source (Beamline 1-BM), a U.S. DOE Office of Science User Facility operated for the DOE Office of Science by Argonne National Laboratory under contrast NO. DE-AC02-06CH11357. TEM analysis was conducted in Electron Microscopy Facility and Proximal Probes Facility of the Center for Functional Nanomaterials, which is a U.S DOE Office of Science User Facility, at Brookhaven National Laboratory under contrast NO. DE-SC0012704. SIMS analysis is in collaboration of EAG laboratories. Joint Photon Sciences Institute at Stony Brook University provided partial support for travel and subsistence at the Advanced Photon Source. The authors would also like to thank Dr. James Quinn from Department of Materials Science and Chemical Engineering at Stony Brook University for the assistance in the SEM analysis.

References

[1] H. Wu, J. Spinelli, P. Konkapaka, M. Spencer, Rapid growth of bulk GaN crystal using GaN powder as source material, MRS Online Proceedings Library Archive 892 (2005).

[2] D. Siche, D. Gogova, S. Lehmann, T. Fizia, R. Fornari, M. Andrasch, A. Pipa, J. Ehlbeck, PVT growth of GaN bulk crystals, J. Cryst. Growth 318(1) (2011) 406-410.

[3] M. Aoki, H. Yamane, M. Shimada, S. Sarayama, F.J. DiSalvo, GaN single crystal growth using high-purity Na as a flux, J. Cryst. Growth 242(1-2) (2002) 70-76.

[4] R. Dwiliński, R. Doradziński, J. Garczyński, L. Sierzputowski, A. Puchalski, Y. Kanbara, K. Yagi, H. Minakuchi, H. Hayashi, Excellent crystallinity of truly bulk ammonothermal GaN, J. Cryst. Growth 310(17) (2008) 3911-3916.

[5] T. Hashimoto, F. Wu, J.S. Speck, S. Nakamura, Ammonothermal growth of bulk GaN, J. Cryst. Growth 310(17) (2008) 3907-3910.

[6] H.P. Maruska, J. Tietjen, The preparation and properties of vapor deposited single crystalline GaN, Appl. Phys. Lett. 15(10) (1969) 327-329.

[7] T. Nakamura, K. Motoki, GaN substrate technologies for optical devices, IEEE, 2013, p. 2221.

[8] B. Raghothamachar, Y. Liu, H. Peng, T. Ailihumaer, M. Dudley, F.S. Shahedipour-Sandvik, K.A. Jones, A. Armstrong, A.A. Allerman, J. Han, H. Fu, K. Fu, Y. Zhao, X-ray topography characterization of gallium nitride substrates for power device development, J. Cryst. Growth 544 (2020) 125709.

[9] Y. Liu, B. Raghothamachar, H. Peng, T. Ailihumaer, M. Dudley, R. Collazo, J. Tweedie, Z. Sitar, F.S. Shahedipour-Sandvik, K.A. Jones, Synchrotron X-ray topography characterization of high quality ammonothermal-grown gallium nitride substrates, J. Cryst. Growth 551 (2020) 125903.

[10] Y. Liu, H. Peng, T. Ailihumaer, B. Raghothamachar, M. Dudley, X-ray Topography Characterization of GaN Substrates Used for Power Electronic Devices, J. Electron. Mater. 50(6) (2021) 2981-2989.

[11] K. Motoki, T. Okahisa, S. Nakahata, N. Matsumoto, H. Kimura, H. Kasai, K. Takemoto, K. Uematsu, M. Ueno, Y. Kumagai, Growth and characterization of freestanding GaN substrates, J. Cryst. Growth 237 (2002) 912-921.

[12] B. Raghothamachar, M. Dudley, X-Ray Topography, Mater. Charact., ASM International2019.

[13] Y. Liu, Z. Chen, S. Hu, H. Peng, Q. Cheng, B. Raghothamachar, M. Dudley, Strain mapping of GaN substrates and epitaxial layers used for power electronic devices by synchrotron X-ray rocking curve topography, J. Cryst. Growth 583 (2022) 126559.

[14] J.W. DuMond, Theory of the use of more than two successive X-ray crystal reflections to obtain increased resolving power, Physical Review 52(8) (1937) 872.

[15] Q. Sun, C.D. Yerino, B. Leung, J. Han, M.E. Coltrin, Understanding and controlling heteroepitaxy with the kinetic Wulff plot: A case study with GaN, J. Appl. Phys. 110(5) (2011).